



TITLE:

# On the Two-Stage Aging of Al-Mg-Si Alloys

AUTHOR(S):

MURAKAMI, Yotaro; KOMATSU, Shinya; ONISHI, Takeo

---

CITATION:

MURAKAMI, Yotaro ...[et al]. On the Two-Stage Aging of Al-Mg-Si Alloys. Memoirs of the Faculty of Engineering, Kyoto University 1969, 31(1): 130-159

ISSUE DATE:

1969-03-25

URL:

<http://hdl.handle.net/2433/280768>

RIGHT:

## On the Two-Stage Aging of Al-Mg-Si Alloys

By

Yotaro MURAKAMI\*, Shinya KOMATSU\*\* and Takeo ONISHI\*\*\*

(Received September 30, 1968)

The two-stage aging effect in three Al-Mg-Si alloys containing 0.5, 1.0 and 1.5% Mg<sub>2</sub>Si respectively is investigated by electrical resistivity measurements, tensile tests and electron microscopy. The critical temperature for homogeneous nucleation of precipitates exists between 160 and 200°C for an 1.0% Mg<sub>2</sub>Si alloy, and for an 1.5% Mg<sub>2</sub>Si alloy between 200 and 260°C. The Temperatures are also corresponding to the highest temperatures for the resistivity increase respectively.

The slight decrease in resistivity perhaps due to redissolution of clusters is observed for 0.5% Mg<sub>2</sub>Si alloy in the initial stage of isothermal aging at a low temperature.

The activation energy  $E_s$  for migration of solute atoms in the fast reaction is estimated as 0.77 eV for all three alloys in good agreement with the values reported for a 1.4% Mg<sub>2</sub>Si alloy. The deleterious effect of two-stage aging is observed in only limited cases, though it appears unfortunately often in practice. The whole effect of two-stage aging appears to be explained only by the stability of clusters or zones formed during preaging. The conservation in zone number is not observed.

The nucleation or stabilization of clusters which takes place during heating to aging temperature must be considered not only for quenching effect but also for two-stage aging effect.

### Introduction

The ternary equilibrium diagram of Al-Mg-Si system involves the quasibinary system of Al-Mg<sub>2</sub>Si. Age-hardenable Al-Mg-Si alloys are widely employed for constructional material because of the easiness in extrusion and other favorable properties.

The precipitation sequence of this alloy has been clarified by X-ray technique<sup>1,2,3)</sup> and electron microscopy<sup>4,5)</sup>, as according to Kelly and Nicholson<sup>19)</sup>, needle-shaped zone → needle shaped internally ordered zone → β' transition phase → β (Mg<sub>2</sub>Si) equilibrium phase.

The zone in this alloy is needle-shaped one parallel to <100> direction of the Al

---

\* Department of Metallurgy.

\*\* formerly Department of Metallurgy, is now at Department of Metallurgy, Faculty of Engineering, Osaka University.

\*\*\* formerly graduate student, is now at Kawasaki Iron and Steel Industry Co. Ltd., Chiba.

matrix, and has coherency strain around the needles<sup>6)</sup>. The  $\text{Mg}_2\text{Si}$  of the equilibrium phase has the anti-isomorphous  $\text{CaF}_2$  structure<sup>29)</sup>.

Similarly to many Al rich alloys, quasibinary Al- $\text{Mg}_2\text{Si}$  alloys show the increase in resistivity during low temperature aging as clarified by Panseri and Federighi<sup>12)</sup>. They treated the transition time between fast and slow reactions, and calculated the activation energy for solutes migration as 0.75eV. They also considered that there was a strong binding energy between zones and vacancies. Lutts<sup>3)</sup> found that the less ordered zones involving vacancies appeared at the initial stage, then the ordered structure was developed and concentration of vacancies in zones decreased with advanced aging. His results are very important for the consideration of the stability of zones.

Because the effect of the two-step aging is a very important problem in commercial practice, many studies concerning this effect have been carried out in some Al alloy systems<sup>6-11,13)</sup>. In Al- $\text{Mg}_2\text{Si}$  alloys containing more than 0.9 %  $\text{Mg}_2\text{Si}$ , the storage at room temperature before artificial aging results in mechanical properties inferior to those aged immediately after quenching. On the contrary, in Al-Zn-Mg alloys, the storage at room temperature gives a favorable effect.

Pashley et al<sup>7)</sup> explained semi-quantitatively the whole effects of two step aging by the stability of clusters formed during preaging. They expressed the stability of clusters at the final aging temperature  $T_2$  as a function of cluster size and supersaturation of matrix, and gave an explanation for four cases of aging temperatures corresponding to  $T_1$  and  $T_2$  at upper and lower side of  $T_{1\text{min}}$  and  $T_c$  respectively. Here,  $T_{1\text{min}}$  is the temperature at which no cluster can grow to attain the size stable at  $T_2$ , and  $T_c$  is the temperature at which the transition from homogeneous nucleation to heterogeneous nucleation takes place. The deleterious effect of two-step aging on the strength is considered to occur in the critical case where the supersaturation is lowered by rather slow dissolution of the fine cluster and the stabilization and proceeding of growth of the clusters is reduced.

Panseri and Federighi<sup>12)</sup> showed the evidence for redissolution of zones smaller in size and growth of the remaining larger zones, by the measurement of electrical resistivity with isothermal two-step aging. They explained two-step aging effect as the strengthening by internally ordered zones proposed by Lutts<sup>3)</sup>.

Lorimer and Nicholson<sup>13)</sup> discussed the favorable effect of two step aging on the age-hardening in an Al-Zn-Mg in terms of the nucleation of the transition phase aided by the zones larger than a critical size. They identified  $T_c$  to the solvus temperature for zones and considered that the size and number of precipitates after final aging can be controlled by pre-aging at a lower temperature. Asano and

Hirano<sup>15,25)</sup> studied two-stage aging characteristics in an Al-5wt% Zn-1wt% Mg alloy by a calorimetric method. The two-stage aging behaviors are shown clearly to be explained in terms of the difference in the number of the G.P. zones at pre- and final aging temperatures by applying Becker's nucleation theory. The model was extended to Al-Mg-Si alloys containing 0.9 and 1.4% Mg<sub>2</sub>Si. Although this model is very favorable for explaining two-stage aging of Al-Zn-Mg alloy system, there seems to be some difficulties in applying to Al-Mg-Si alloys. In these alloys, increment in resistivity at low temperature aging is higher than that of high temperature. This tendency is understood as, whatever the cause of resistivity maxima may be, the number of zones becomes larger at lower aging temperatures between 20 and 170°C as shown latter in Fig. 3.

If it is assumed that only large clusters can proceed to grow at  $T_2$ , there occurs another question as to why it is estimated the relation between zone number and aging temperature from the result of isochronal resistivity measurements, because the resistivity is increased by only relatively small zones. Furthermore, though the deleterious effect of two-step aging appears in the specimen pre-aged at room temperature for more than several days, Panseri's isochronal curve is obtained by aging for merely 2 min at each temperature elevating in steps of 20°C<sup>12)</sup>. It is thought that the assumption about the conservation of zone number to  $T_2$ , may not be pertinent in this case where the change in zone number at  $T_2$  after pre-aging must be considered.

It is well known that the rate of clustering is very high immediately after quenching and even during cooling the cluster may be formed to some extent. Also during heating, clustering may occur and the resultant clusters will be more stable than those formed during cooling. When widely defined, the aging immediately after quenching to a low temperature must be considered as a kind of two-step aging. Then, in the present work, it is attempted to explain inoculation effect by quenching together with the effect of two-step aging.

At first, the kinetics of zone formation is investigated by measurements of electrical resistivity and proof stress for low temperature aging, and by measurements of proof stress and electron microscopy for high temperature aging. When the effect of two-step aging is discussed, the stability of zones at elevated temperatures must be considered. The solute supersaturation will be easily controlled by changing the alloy composition. It is also interesting to investigate the improved mechanical properties in the alloy of concentration lower than 0.9% Mg<sub>2</sub>Si reported by Zoller and Ried<sup>16)</sup>. Then, in this work, the aging behaviours of Al-Mg-Si alloys are investigated with three alloys containing 0.5, 1.0 and 1.5% Mg<sub>2</sub>Si.

### Experimental Procedure

The alloys were chosen to contain 0.5, 1.0 and 1.5%  $Mg_2Si$  respectively. The ingots of  $20 \times 100 \times 150$  mm for foil and  $20 \times 20 \times 300$  mm for wire were prepared from 99.99% purity Al, Mg and Si. The wire was prepared from cast ingots which had been homogenized at  $550^\circ C$  for 12 hrs, hot rolled to about 5 mm in diameter and cold drawn for tensile tests to 1.1 mm and for electrical resistivity measurements to 0.75 mm in diameter. For electron microscopy the foil of 0.15 mm thick was prepared by rolling after the same homogenizing treatments as above. The chemical compositions of alloys were shown in Table 1.

Table 1. Analysed composition of alloys. (wt.%)

Alloy Mark	Mg	Si	$Mg_2Si$	Excess Mg
0.5 $Mg_2Si$	0.34	0.18	0.49	0.03
1.0 $Mg_2Si$	0.67	0.36	0.98	0.05
1.5 $Mg_2Si$	0.97	0.52	1.42	0.07

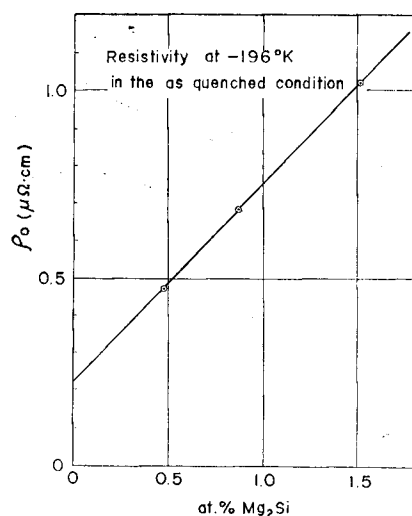


Fig. 1. The relation between the concentrations of solute atoms and the resistivity at liquid nitrogen temperature immediately after the quenching to  $-20^\circ C$  from  $570^\circ C$ .

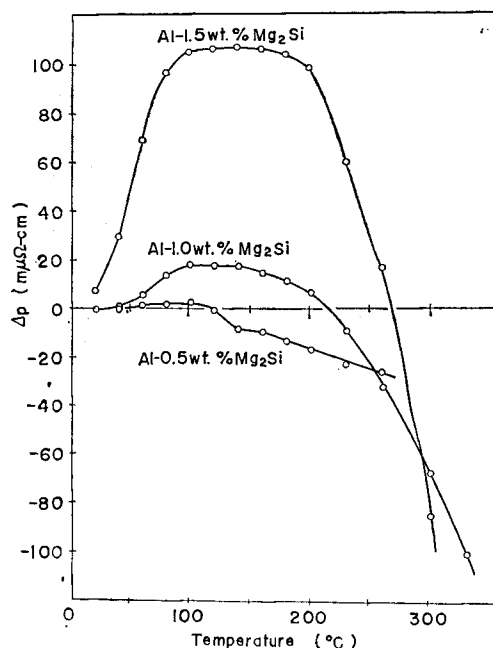


Fig. 2. Isochronal changes in resistivity of three alloys aged at each temperature for 1 min. after quenching to  $-20^\circ C$  from  $570^\circ C$ .

The specimens were solution-treated at 570°C for 30 min and then quenched to  $-20^{\circ}\text{C}$  brine, or directly to oil bath, whose temperature was regulated to aging temperatures. Aging temperatures were chosen between the range from  $0^{\circ}\text{C}$  to  $340^{\circ}\text{C}$  at intervals of 20 or  $30^{\circ}\text{C}$ . As for aging bath, water below  $20^{\circ}\text{C}$ , sesame oil for  $20-100^{\circ}\text{C}$ , silicone oil for  $100-200^{\circ}\text{C}$  and salt bath of  $\text{KNO}_2\text{-NaNO}_2$  above  $200^{\circ}\text{C}$  were employed, respectively.

Other details for resistivity measurement and tensile test were described previously<sup>22)</sup>. For the direct observation by transmission electron microscopy, the foil of  $0.15 \times 15 \times 35$  mm was aged and electrolytically thinned in ethanol-10% perchloric acid, then observed by J.E.M-12 at 120 KV.

### Results and Discussion

The specimen was quenched by dropping into brine of  $-20^{\circ}\text{C}$  after the solution treatment at  $570^{\circ}\text{C}$  for 30 min. After aging, resistance was measured at liquid  $N_2$  temperature. The size factor was calculated for each specimen. The results are expressed as the change in resistivity for the as-quenched value.

The resistivity of three alloys at liquid  $N_2$  temperature in as-quenched states ( $\rho_0$ ) is shown in Fig. 1 as the function of solute concentration. There is very

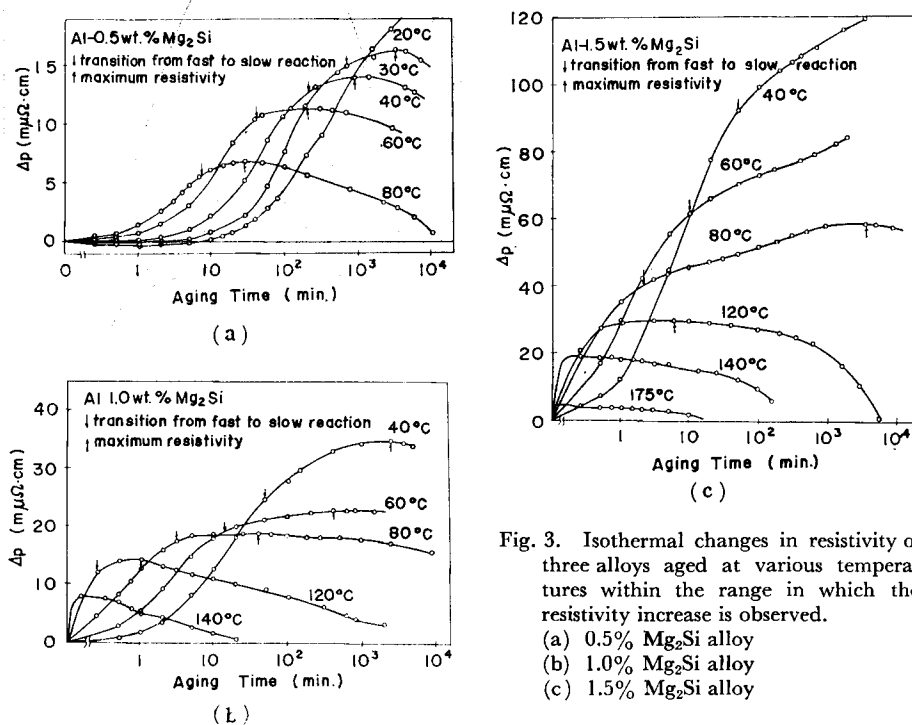
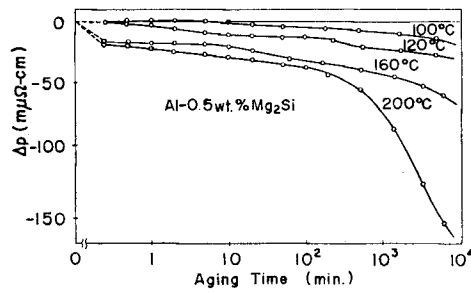


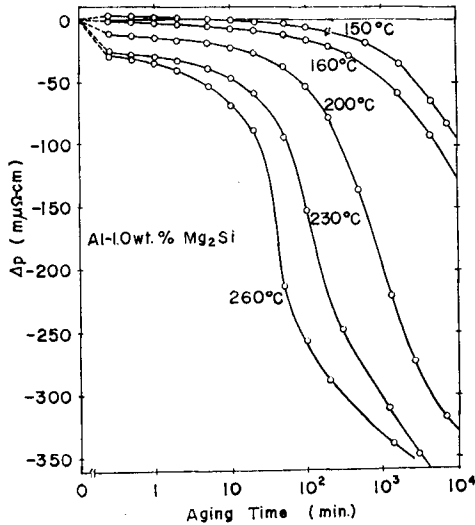
Fig. 3. Isothermal changes in resistivity of three alloys aged at various temperatures within the range in which the resistivity increase is observed.  
 (a) 0.5%  $\text{Mg}_2\text{Si}$  alloy  
 (b) 1.0%  $\text{Mg}_2\text{Si}$  alloy  
 (c) 1.5%  $\text{Mg}_2\text{Si}$  alloy

good agreement with the linear relation of  $\rho_0 = \{\rho_{Al}(0.22) + 0.53 C(\text{at. } \%)\} \mu\Omega \text{ cm}$ . Figure 2 shows the results of isochronal aging for 1 min. at each temperature at interval of 20 or 30°C, in the range from 20°C to 340°C. For 1.5% Mg<sub>2</sub>Si alloy, there is a good agreement with Panseri's observation<sup>12)</sup>. Namely, the resistivity increases with temperature up to 100°C, and holds an almost constant value till the rapid decrease above 200°C.

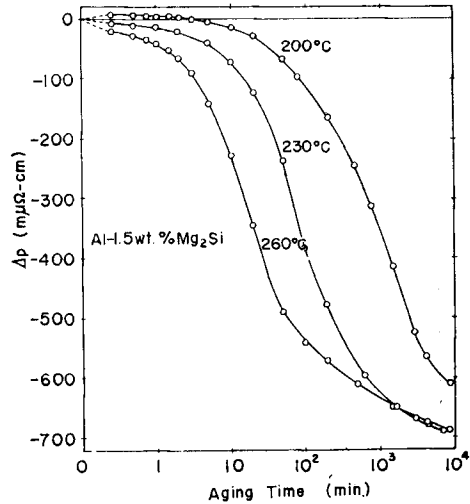
It may be seen from this plateau that zones or clusters formed once at a lower temperature are stable up to a rather high temperature. The rapid decrease begins at 160°C in 1.0% Mg<sub>2</sub>Si alloy and at 120°C in 0.5% Mg<sub>2</sub>Si alloy. These temperatures agree with the previous results which are 200°C for 1.4%<sup>12)</sup> and 160°C for 0.89% Mg<sub>2</sub>Si alloy<sup>14)</sup>. Comparing the value of resistivity in Fig. 2 with that of isothermal aging, the former is always larger than the latter, because the additive aging will give an inoculation effect and zones will be increased in number<sup>12)</sup>.



(a)



(b)



(c)

Fig. 4. Same as Fig. 3, but the aging temperature is higher than the limit of resistivity increase.

- (a) 0.5% Mg<sub>2</sub>Si alloy
- (b) 1.0% Mg<sub>2</sub>Si alloy
- (c) 1.5% Mg<sub>2</sub>Si alloy

Besides, the peak value in isochronal aging as the function of solute concentration is not linear.

The isothermal curves of the temperatures at which the resistivity increases are shown in Fig. 3(a), (b), and (c) for three alloys as a scale of log time. In Fig. 4, the isothermal curves at higher temperatures are shown in the same way as Fig. 3. The increase in resistivity becomes larger the higher is the solute concentration when compared with that of at the same temperature and the same period, and after a long aging period becomes smaller, the higher is the temperature. This observation may be qualitatively explained in terms of larger number of zones with higher solute concentration and lower aging temperature.

The resistivity maximum  $\Delta\rho_m$  is observed at time  $t_m$ , similarly as in other Al alloys, though the peak becomes rather flat in higher concentration of solute. It is notable that  $t_m$  becomes larger in the alloy of higher concentration when compared at the same aging temperature. This trend is in contrast to the usual knowledge about the kinetics in precipitation and is very interesting when it is related to the observation about isochronal aging shown in Fig. 2. The resistivity maximum becomes observable at the lower temperature, the lower is the solute concentration.

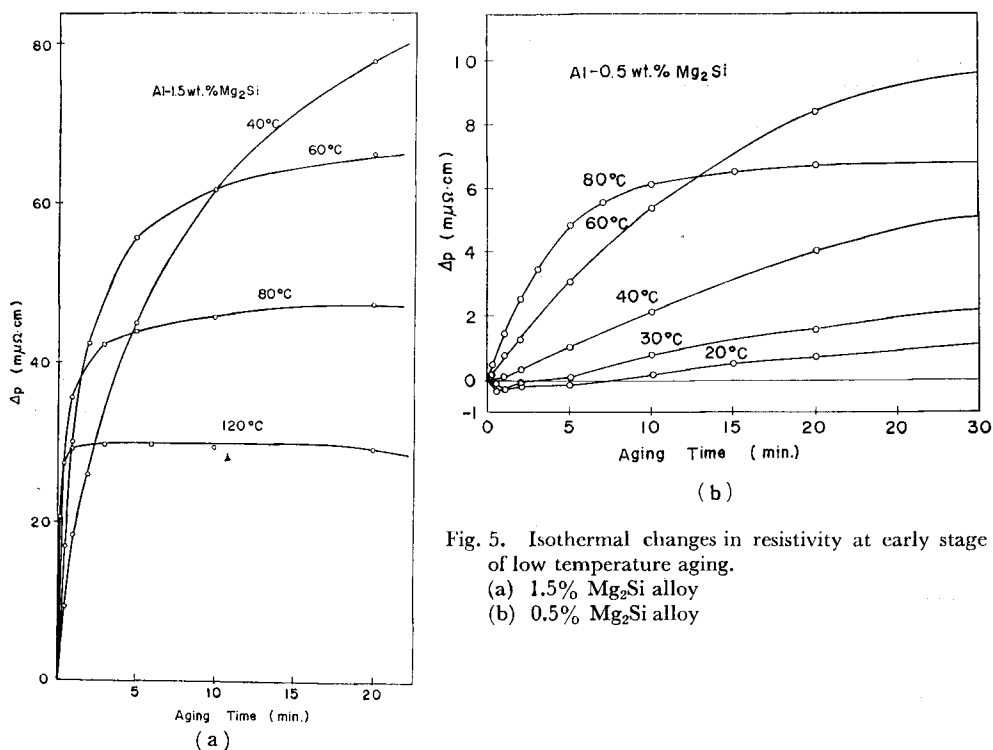


Fig. 5. Isothermal changes in resistivity at early stage of low temperature aging.  
 (a) 1.5% Mg<sub>2</sub>Si alloy  
 (b) 0.5% Mg<sub>2</sub>Si alloy



Figure 5 shows the variation of resistivity, when time is expressed linearly. The transition between initial fast reaction and following slow reaction occurs very clearly at a time  $t_s$ , especially in the temperature range from 40°C to 80°C. In the 0.5% Mg<sub>2</sub>Si alloy (Fig. 5(b)), the decrease in resistivity is observed at the initial stage of aging at 20°C and 30°C. This phenomenon may be explained by the re-dissolution of very small and unstable clusters formed during quenching or at the quenching temperature, -20°C.

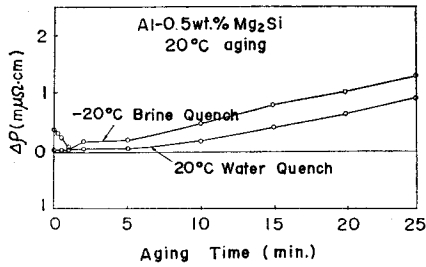


Fig. 6. The comparison of isothermal change in resistivity at 20°C for Al-0.5% Mg<sub>2</sub>Si alloy quenched into -20°C and 20°C respectively.

The isothermal curves at 20°C after quenching to -20°C and direct quenching to 20°C are shown in Fig. 6. The decrease in resistivity is not observed in the specimen quenched directly to 20°C. This decrease disappears in the alloy of higher concentration and/or at higher temperature, because the resistivity increase at the large rate of formation of zones and/or the large number of zones exceeds the decrease by re-dissolution of clusters. It is also considered that the nucleation process may be necessary for the zone formation in this alloy system, similarly as that in Al-Cu

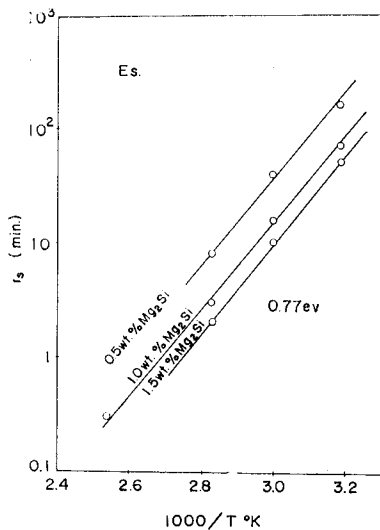


Fig. 7. The relation between the reciprocal of absolute aging temperature and the transition time ( $t_s$ ) from fast to slow reaction.

<sup>26,27)</sup> and Al-Zn-Mg alloys<sup>28)</sup> reaged after reversion. The values of transition time  $t_s$ , and resistivity increment  $\Delta\rho_s$  are shown in Table 2 together with the value of proof stress. The both value of  $t_s$  and  $\Delta\rho$  decrease as the temperature is raised, while the value of proof stress remains nearly equal. Figure 7 shows the relation between  $\log t_s$  and reciprocal of the absolute aging temperatures. The points for each alloy lie on a straight line respectively, and the values of activation energy for fast reaction  $E_s$  are calculated from the Arrhenius-type equation as 0.77eV for all three alloys of different compositions. The value of activation energy is in good agreement with the result of Panseri and Federighi<sup>12)</sup>,  $0.75 \pm 0.03$ eV. It is clear from Fig. 7 and Table 2 that the transition between fast and slow reaction occurs earlier with increasing solute concentration of alloys. However, as shown

Table 2. The comparison of resistivity increment and proof stress at the transition points of fast and slow reaction in the resistivity change by isothermal aging.

alloy	aging temp. (°C)	$t_s$ (min.)	$\Delta\rho_s$ ( $m\mu\Omega$ cm)	proof stress (Kg/mm <sup>2</sup> )
0.5% Mg <sub>2</sub> Si	40	160	12.1	4.6
	60	40	10.4	4.6
	80	8	5.8	5.2
1.0% Mg <sub>2</sub> Si	40	70	21.4	5.2
	60	16	19.4	5.1
	80	3	17.2	5.1
1.5% Mg <sub>2</sub> Si	40	50	92.4	8.1
	60	10	62.5	8.0
	80	2	40.0	7.6

Table 3. The comparison of resistivity increment and proof stress at the maxima in the resistivity change by isothermal aging.

alloy	aging temp. (°C)	$t_{\max}$ (min.)	$\Delta\rho_{\max}$ ( $m\mu\Omega$ cm)	proof stress (Kg/mm <sup>2</sup> )
0.5% Mg <sub>2</sub> Si	30	3200	16.4	6.2
	40	900	14.2	5.3
	60	220	11.2	5.8
	80	30	6.8	5.2
1.0% Mg <sub>2</sub> Si	40	2400	35.4	6.0
	60	400	22.6	6.2
	80	40	28.8	5.8
	120	1.0	14.2	5.5
1.5% Mg <sub>2</sub> Si	80	2500	59.0	13.7
	120	6	29.6	8.8

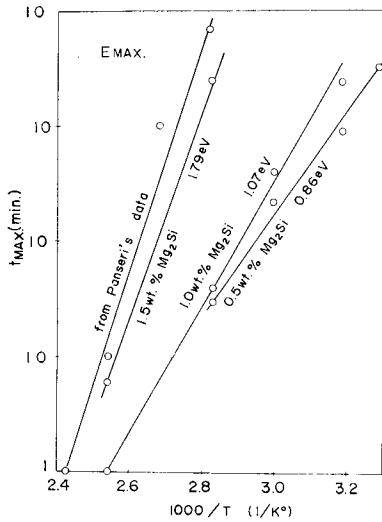


Fig. 8. The relation between the reciprocal of absolute aging temperature and the time of maximum resistivity ( $t_{\max}$ ).

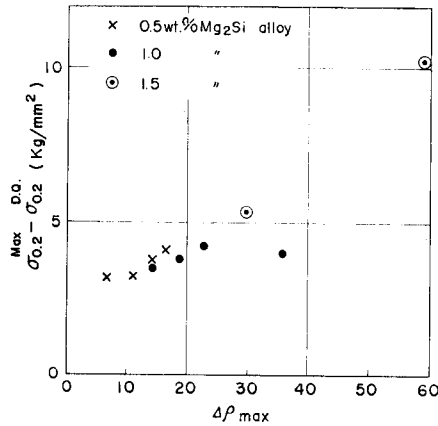


Fig. 9. The relation between  $\Delta\rho_{\max}$  and  $\Delta\sigma$  ( $\sigma - \sigma_{D.Q.}$ ).

in Table 3 this tendency is not observed in the case of resistivity maxima, though the value of  $t_{\max}$  becomes less with higher aging temperature. For trial, the log  $t_{\max}$  values are plotted against the reciprocal of the absolute aging temperature in Fig. 8. Panseri's data are also plotted in Fig. 8 and show a good agreement with present results of 1.5 %  $Mg_2Si$  alloy. Apparently, the points lie on a straight line for each alloy and the activation energy  $E_{\max}$  calculated assuming the validity of Arrhenius-type equation, are larger in the alloy of higher solute concentration. For all three alloys  $E_{\max}$  is larger than  $E_s$ . This observation will support the existence of strong binding between vacancies and zones suggested by Lutts<sup>3)</sup> and Panseri et al<sup>12)</sup>. Namely, the growth of zones after  $t_s$  may progress under very low concentration of vacancies and the apparent activation energy involves not only migration energy of solute but also the energy necessary to release vacancies from zones. The reason for the less  $t_{\max}$  in the alloy of lower solute concentration will be given by the larger value of  $\Delta\rho_s/\Delta\rho_{\max}$ . The value of proof stress corresponding to  $t_{\max}$  becomes less the higher is the aging temperature. In Fig. 9,  $\Delta\sigma_{0.2}^{\max}$  is plotted against  $\Delta\rho_{\max}$ . If the proof stress immediately after direct quenching (in Table 4 and 5) may be taken as the reference value, a certain linear relation is observed. This fact is, at least, consistent with the assumption<sup>24)</sup> that the change in resistivity at maximum is due to the change in number of zones.

Table 4. The proof stress of the Al-1.0% Mg<sub>2</sub>Si alloy after two-step aging. (Kg/mm<sup>2</sup>)

pre-heat treatments	no final heat treatment	260°C 30 min.	200°C 5 hrs.	160°C 1 day
-20°C Q.	3.3	11.4	14.8	12.9
D. Q.	2.0	2.2	4.6	9.8
40°C 1 w.	6.0	12.8	17.3	15.5
120°C 1 w.	10.6	8.0	18.1	17.5

Table 5. The proof stress of the Al-1.5% Mg<sub>2</sub>Si alloy after two-step aging. (Kg/mm<sup>2</sup>)

pre-heat treatments	no final heat treatment	260°C 30 min.	200°C 5 hrs.	260°C 1 day
-20°C Q.	5.5	20.7	25.7	24.4
D. Q.	3.5	15.1	24.1	24.5
40°C 1 w.	11.4	18.0	25.5	21.5
120°C 1 w.	20.2	18.9	26.0	26.0

It is necessary to know the change in mechanical properties with aging immediately after quenching, before the effect of double aging is discussed. In Al-Zn-Mg alloys<sup>8,13</sup>, it has been clarified that a critical temperature exists between the homogeneous nucleation and heterogeneous nucleation of precipitates. This cri-

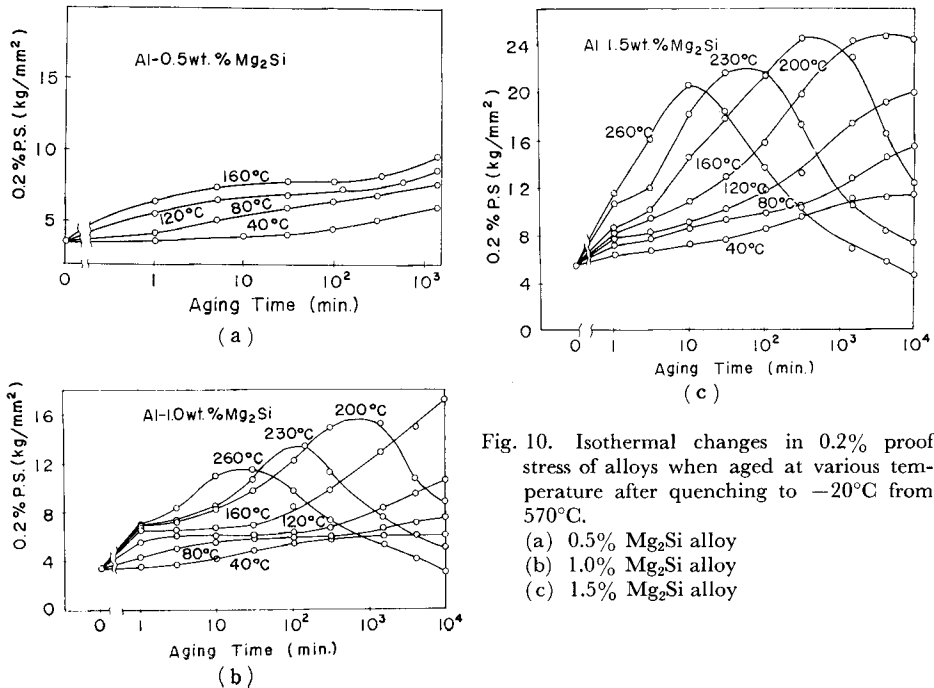


Fig. 10. Isothermal changes in 0.2% proof stress of alloys when aged at various temperature after quenching to  $-20^{\circ}\text{C}$  from  $570^{\circ}\text{C}$ .

- (a) 0.5% Mg<sub>2</sub>Si alloy
- (b) 1.0% Mg<sub>2</sub>Si alloy
- (c) 1.5% Mg<sub>2</sub>Si alloy

tical temperature was also reported as 190°C–220°C in the Al-1.2% Mg<sub>2</sub>Si alloy by Pashley et al<sup>7)</sup>. Then the age-hardening was investigated to clarify this temperature. At first, the specimens were quenched into -20°C brine and isothermally aged at various temperatures. Isothermal age-hardening curves are shown in Fig. 10 where the proof stress is plotted against log time. The increase in proof stress becomes larger the higher is the solute concentration similarly to that of the resistivity. Age-hardening appears to take place in two stages, which is especially apparent in 0.5% and 1.0% Mg<sub>2</sub>Si alloy aged below 160°C as shown in Fig. 10(a) and (b). However, these stages disappear when time is expressed linearly. The maximum value occurs for time  $t_{\sigma_{max}}$  in 1.0% and 1.5% Mg<sub>2</sub>Si alloys above 200°C. The value of  $t_{\sigma_{max}}$ , contrary to the case of resistivity, becomes less as the solute concentration increase. At the aging temperatures lower than ca. 100°C the rate of decomposition of solid solution may be influenced by excess concentration of vacancies. There may be no influence of vacancy above 200°C except to facilitate the nucleation of precipitates. The isothermal curves above 200°C are similar to each other, in spite of the results mentioned above about the stability limit of zones. Figure 11 shows the effect of direct quenching of the aging temperature on following age-

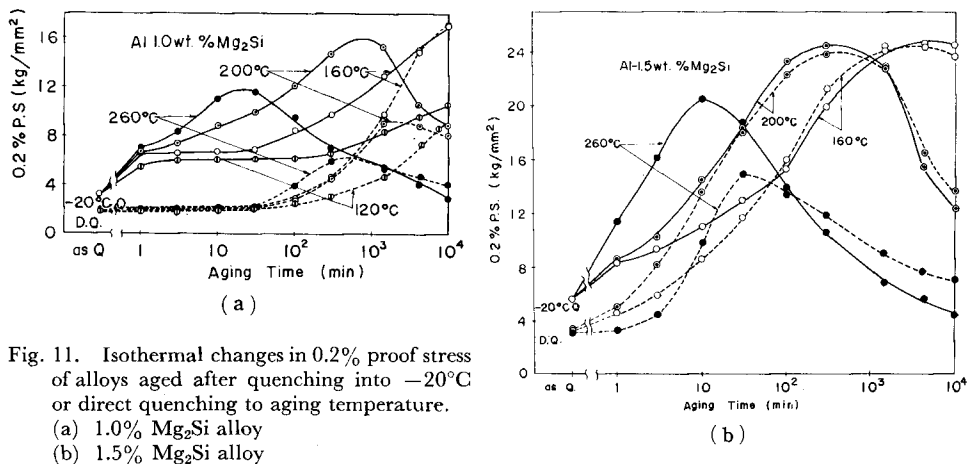


Fig. 11. Isothermal changes in 0.2% proof stress of alloys aged after quenching into -20°C or direct quenching to aging temperature.  
 (a) 1.0% Mg<sub>2</sub>Si alloy  
 (b) 1.5% Mg<sub>2</sub>Si alloy

hardening. The solid and broken lines show isothermal change in proof stress after -20°C and direct quenching, respectively. The value of proof stress immediately after -20°C quenching is larger than that of after direct quenching. This excess value is due to the clusters formed at quenching temperature and containing large number of vacancy. In aging below 160°C with 1.0% Mg<sub>2</sub>Si alloy or 200°C with 1.5% Mg<sub>2</sub>Si alloy, the curve of direct quenching attains the same value as that of -20°C quenching. The remarkable effect is observed in aging above 200°C

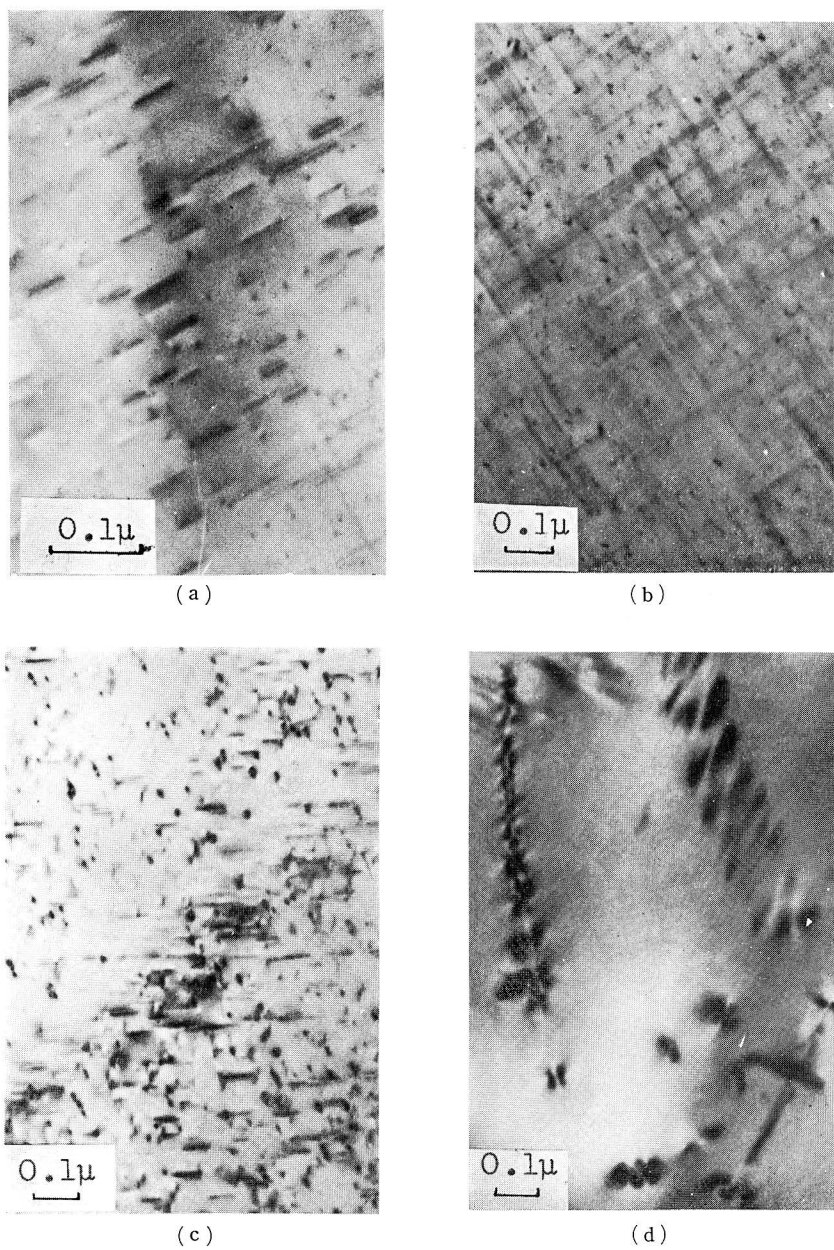


Photo. 1. The effect of quenching on the precipitation in Al-1.0% Mg<sub>2</sub>Si alloy.  
(a) quenched to  $-20^{\circ}\text{C}$  brine, and aged at  $160^{\circ}\text{C}$  for 1 day.  
(b) quenched to  $-20^{\circ}\text{C}$  brine, and aged at  $200^{\circ}\text{C}$  for 10 hrs.  
(c) directly quenched to the aging temperature of  $160^{\circ}\text{C}$  and aged for 1 day.  
(d) directly quenched to the aging temperature of  $200^{\circ}\text{C}$  and aged for 10 hrs.

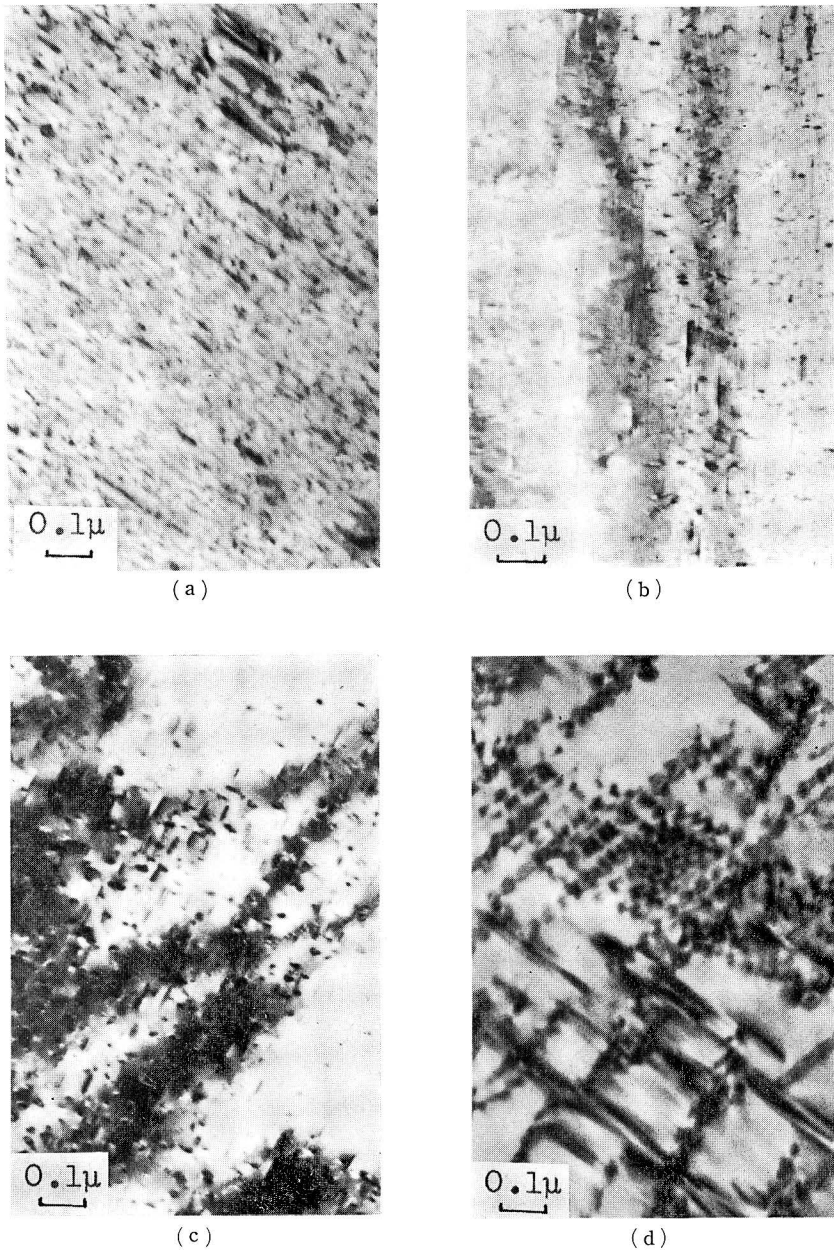


Photo. 2. The effect of quenching on the precipitation in Al-1.5% Mg<sub>2</sub>Si alloy.  
 (a) quenched to  $-20^{\circ}\text{C}$  brine, and aged at  $200^{\circ}\text{C}$  for 5 hrs.  
 (b) quenched to  $-20^{\circ}\text{C}$  brine, and aged at  $260^{\circ}\text{C}$  for 10 min.  
 (c) directly quenched to the aging temperature of  $200^{\circ}\text{C}$ , and aged for 5 hrs.  
 (d) directly quenched to the aging temperature of  $260^{\circ}\text{C}$ , and aged for 30 min.

with 1.0%  $\text{Mg}_2\text{Si}$  alloy. Age-hardening takes place also in specimens directly quenched, but the maximum value in the directly quenched specimen is much less than that of specimens quenched to  $-20^\circ\text{C}$ . It is clear that the transition temperature  $T_c$  exists between  $160^\circ\text{C}$  and  $200^\circ\text{C}$  for 1.0 %  $\text{Mg}_2\text{Si}$  alloy and for 1.5%  $\text{Mg}_2\text{Si}$  alloy between  $200^\circ\text{C}$  and  $260^\circ\text{C}$  at which the aspect of precipitation varies pronouncedly. The acceleration of age-hardening above transition temperature after quenching to low temperature, may be explained in terms of the reduction in diffusion distance due to increased number of zones or nuclei. As reported in Al-Zn-Mg alloys<sup>8,13)</sup> the direct quenching leads to a coarser precipitate and a predominant heterogeneous nucleation. This effect is also observed in the present alloys by electron microscopy. Photos. 1 and 2 show the structures after the aging treatments corresponding to maxima in proof stress. It is to be noted that, when specimens are quenched to  $-20^\circ\text{C}$ , there is essentially no difference in structure except coarser distribution in higher aging temperature even above the critical temperature for the stability of zones. Namely, as shown in Fig. 10, the isothermal age-hardening curves resemble each other for above and below the critical temperature. However, when specimens are directly quenched to the temperature above  $T_c$ , the fine precipitates becomes hard to observed, and there are large precipitates heterogeneously nucleated on dislocations. For example, in Photo. 1(d), arrays of precipitates are observed. Thus, we can consider that the nucleation may occur at the temperature lower than  $T_c$  in the case of quenching to  $-20^\circ\text{C}$ .

Undoubtedly, the nucleation is aided by quenched-in vacancies, but its mechanism will be very complicated. Perhaps the aging at upto ca.  $100^\circ\text{C}$  may be accelerated by quenched-in vacancies, but in the alloy containing Mg, the effect of quenching method on the rate of age-hardening becomes hard to recognize<sup>22)</sup>. However, in Al- $\text{Mg}_2\text{Si}$  alloys, although there is an incubation period even when the time is expressed linearly and a delay in aging time corresponding to the maximum proof stress, a remarkable hardening takes place even after direct quenching in contrast to the case of the Al-Zn-Mg alloy<sup>8)</sup>. These results suggest that the diffusion at aging temperatures above  $200^\circ\text{C}$  is not influenced, but the number of zones and consequently the average diffusion distance is influenced by quenching method or concentration of quenched-in vacancies.

The changes in resistivity with isothermal aging at  $80^\circ\text{C}$  after the pre-aging for various periods at  $40^\circ\text{C}$  are shown in Figs. 12 and 13. These agree well with Panzeri's results<sup>12)</sup>. Namely, the resistivity continues to increase above the peak values of  $80^\circ\text{C}$  aging, contrary to Al-Zn alloys<sup>24)</sup>. Further, in Fig. 13, fast and slow reac-



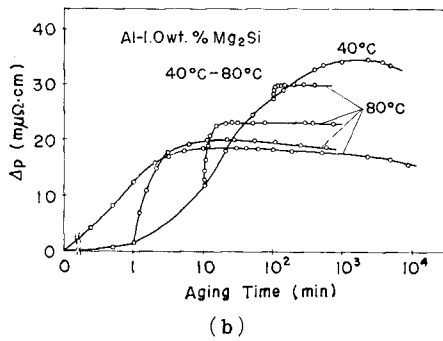
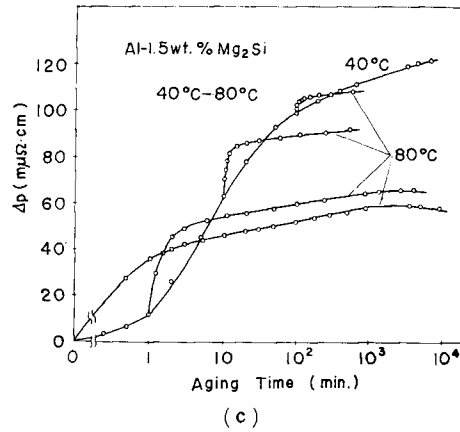
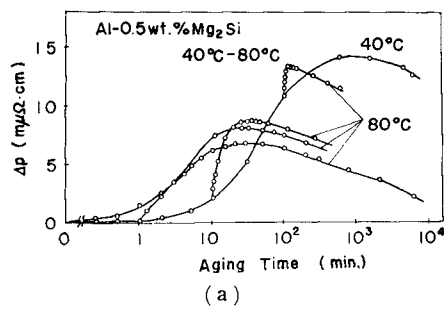


Fig. 12. Isothermal changes in resistivity of alloys aged at 80°C after pre-aging at 40°C for various periods.

- (a) 0.5% Mg<sub>2</sub>Si alloy
- (b) 1.0% Mg<sub>2</sub>Si alloy
- (c) 1.5% Mg<sub>2</sub>Si alloy

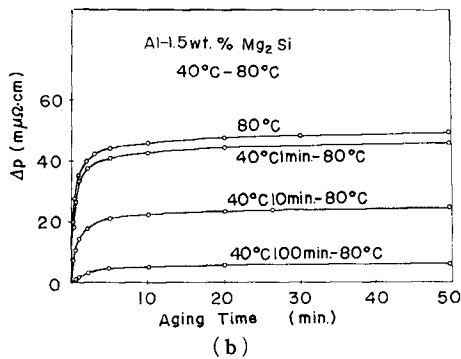
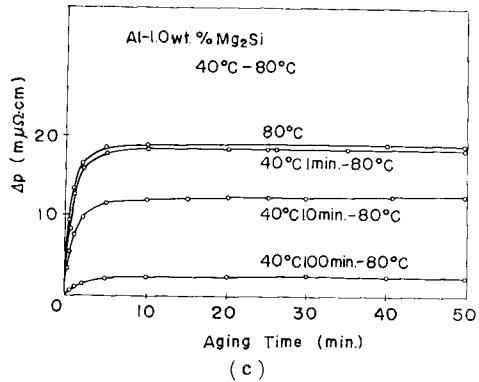
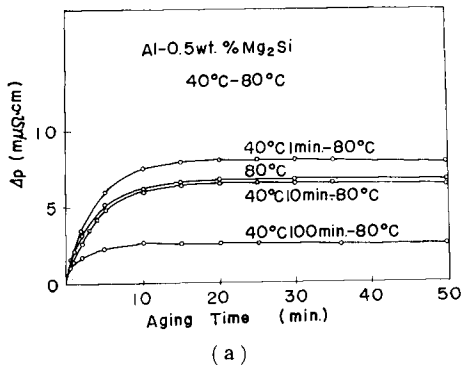
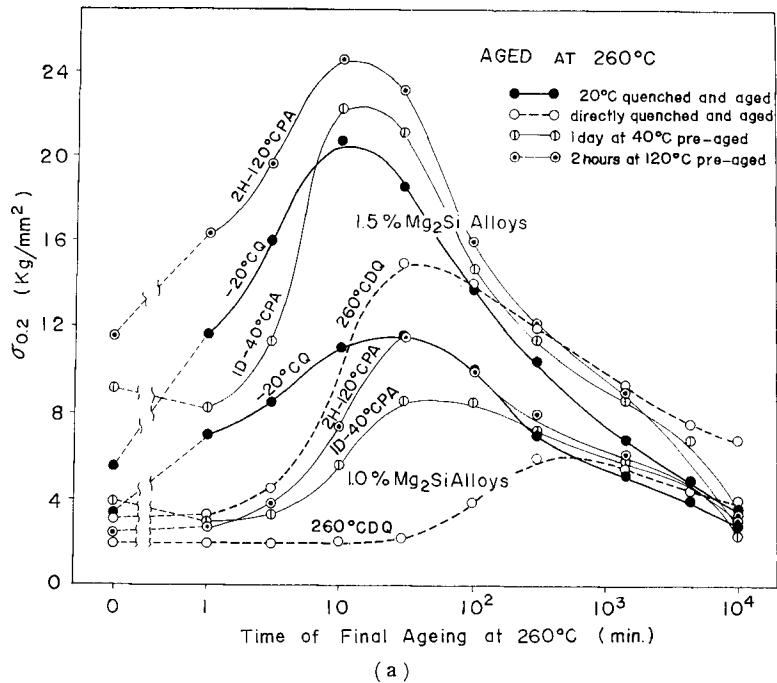


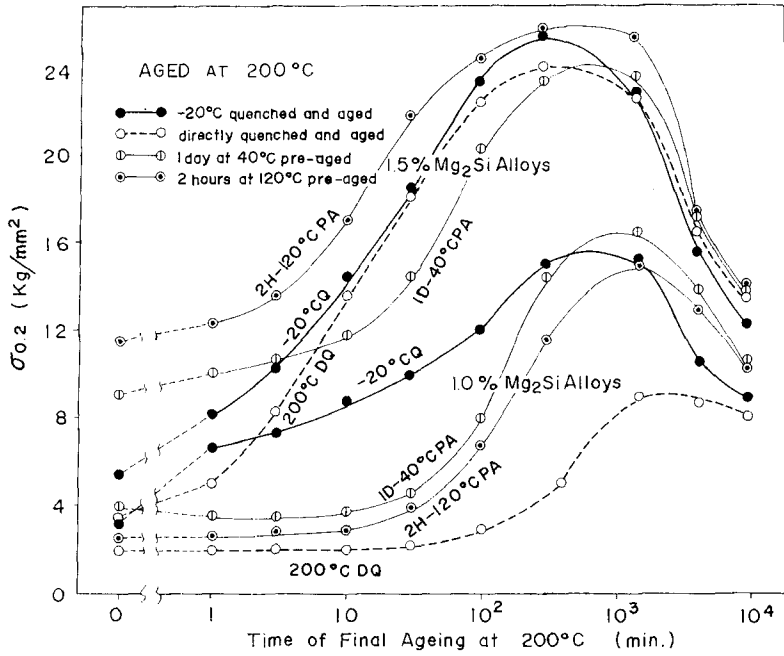
Fig. 13. Same results as Fig. 11. Resistivity increment by 80°C aging after 40°C aging for various periods is plotted on a linear time scale.

- (a) 0.5% Mg<sub>2</sub>Si alloy
- (b) 1.0% Mg<sub>2</sub>Si alloy
- (c) 1.5% Mg<sub>2</sub>Si alloy

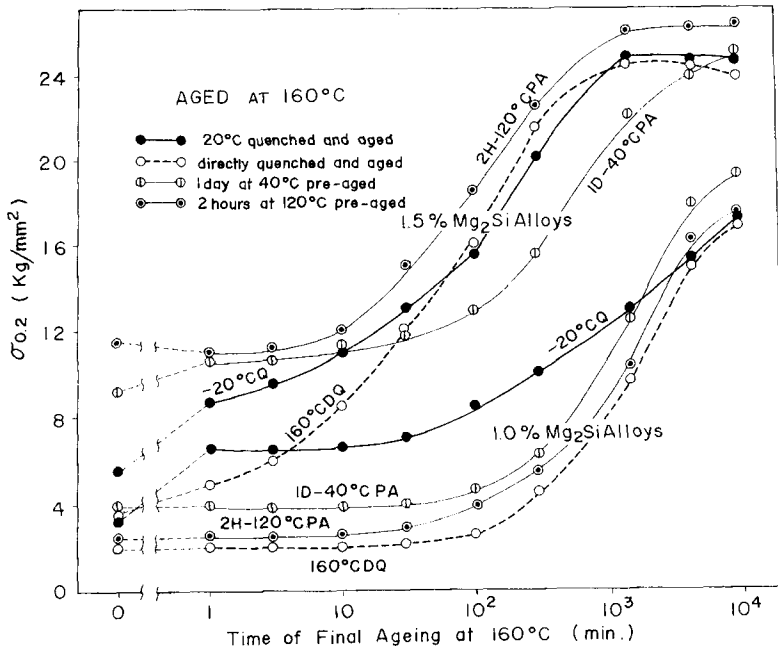
tions are observed even after the pre-aging for 100 min. at 40°C, where almost all movable vacancies should have been annealed out. These results suggest that the zones increase in number after the pre-aging at a lower temperature. There are two additional observations in the 0.5 %  $Mg_2Si$  alloy. A shorter peak time is shown when pre-aged for 1 min. Further, with the decreasing  $Mg_2Si$  content, the increment in resistivity by 80°C aging after the pre-aging is brought closer to that of no pre-aging and, finally in Fig. 13(a) for 0.5 %  $Mg_2Si$  alloy, exceeds the value of simple aging at 80°C. The former observation suggests that the Ostwald ripening takes place in two-step aging, because the decreased distance of solute diffusion does not effect the growth rate of the individual zones and, consequently, the peak can not be explained only by the critical zone size. Thus, the occurrence of resistivity maximum in final aging is partially due to the decrease in zone number. The latter observation is explained by increasing inoculation effect in 80°C aging and/or decreasing rate of aging at 40°C after  $-20^\circ C$  quenching with decreasing alloy concentration.

As already mentioned above, there is a critical temperature  $T_c$  for homogeneous nucleation, which lies between 160 and 200°C in 1.0 %  $Mg_2Si$  alloy, and between 200 and 260°C in 1.5%  $Mg_2Si$  alloy, respectively. In the same temperature range, the resistivity increase becomes not observable when the specimen is quenched to





(b)



(c)

Fig. 14. Effect of various pre-aging treatments on the isothermal changes in 0.2% proof stress at various final aging temperatures. (a) 260°C (b) 200°C (c) 160°C

$-20^{\circ}\text{C}$ . Thus, 160, 200 and  $260^{\circ}\text{C}$  are chosen as final aging temperatures  $T_2$  to be located in both sides of  $T_c$ . As pre-aging temperatures  $T_1$ ,  $40$  and  $120^{\circ}\text{C}$  are employed to give different sizes and numbers of zones. In this case the specimens are quenched directly to the pre-aging temperatures.

It is very important to investigate the effect of some fixed pre-aging treatments on the isothermal aging at  $T_2$ , because the increase or decrease in strength after a two-step aging is sometimes due to the large or small rate of age-hardening. The effects of primary aging at  $40^{\circ}\text{C}$  for 1 day and at  $120^{\circ}\text{C}$  for 2 hrs on the isothermal age-hardening are shown in Fig. 14, together with the curves of isothermal aging after  $-20^{\circ}\text{C}$  quenching and direct quenching.

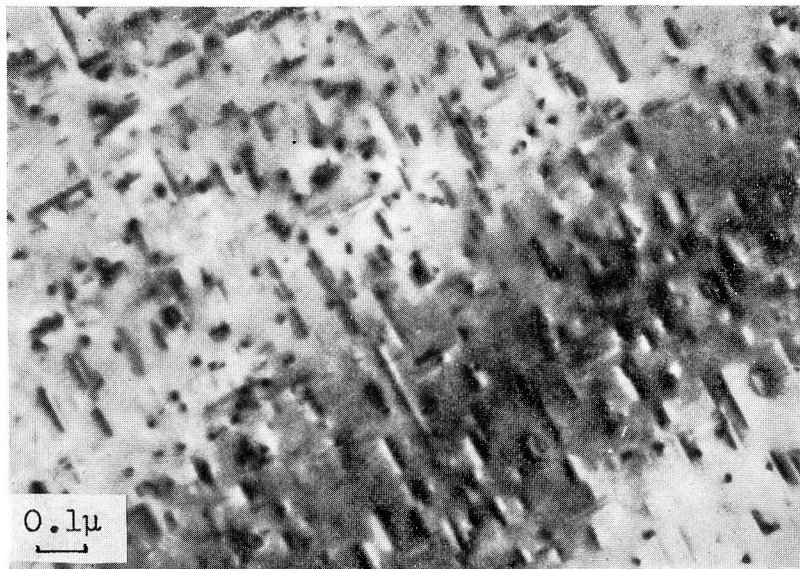
When the 1.5 %  $\text{Mg}_2\text{Si}$  alloy is pre-aged at  $40^{\circ}\text{C}$  for 1 day, the retardation is observed in 160 and  $200^{\circ}\text{C}$ . But there is no difference from  $-20^{\circ}\text{C}$  quenching or direct quenching in the value of maximum proof stress. In final aging at  $260^{\circ}\text{C}$ , the maximum proof stress after pre-aging is larger than that of  $-20^{\circ}\text{C}$  quenching.

The retardation of hardening in the pre-aged specimens becomes clearer in the 1.0 %  $\text{Mg}_2\text{Si}$  alloy than in the 1.5 %  $\text{Mg}_2\text{Si}$  alloy. The maximum proof stress appears later in final aging above  $T_c$ , namely at 200 and  $260^{\circ}\text{C}$ . In  $200^{\circ}\text{C}$  aging of the 1.0%  $\text{Mg}_2\text{Si}$  alloy, the maximum value is raised by the pre-aging at  $40^{\circ}\text{C}$ , but at  $260^{\circ}\text{C}$ , it is less than those of pre-aged at  $120^{\circ}\text{C}$  and after the quenching to  $-20^{\circ}\text{C}$ . Photo. 3 shows the results of direct observation of the effect of pre-aging on the precipitation in 1.0%  $\text{Mg}_2\text{Si}$  alloy after final aging at  $160^{\circ}\text{C}$  for 1 day. When pre-aged at  $120^{\circ}\text{C}$  for 2 hrs (b), the precipitates are larger than those of at  $40^{\circ}\text{C}$  for 1 day, in agreement with the upper curves of pre-aging at  $40^{\circ}\text{C}$  in Fig. 14(c).

In general, the pre-aging gives the larger values in proof stress than those of after direct quenching, except a few cases. For convenience of putting these complicated results in order, the isochronal or isothermal pre-aging followed by fixed treatments of final aging are often used. However, it must be noted that the retardation in age-hardening sometimes gives rise to the decrease in strength after fixed final aging. These retardations are classified into two kinds. One shows the decrease and the other gives nearly equal or higher value in maximum proof stress which appears later than that of  $-20^{\circ}\text{C}$  quenching. The former is explained by the decreased number in nuclei. So far as the retardation in direct quenching is concerned, it is reasonable to understand that the decreased nuclei increase the average diffusion distance of solute atoms and that the total volume of precipitates increases more slowly than that of fast quenching. The retardation after pre-aging may be explained by the dissolution of small zones which occur rather slowly because of the strong bonding between Mg and Si atoms. In the case of less maximum value, the



(a)



(b)

Photo. 3. The effect of pre-aging on the precipitation in Al-1.0% Mg<sub>2</sub>Si alloy aged at 160°C for 1 day.  
(a) pre-aged at 40°C for 1 day.  
(b) pre-aged at 120°C for 2 hrs.

nucleation or stabilization of zones occurring at a temperature lower than  $T_c$  is greatly suppressed by the low degree of supersaturation. On the contrary, when the supersaturation is sufficiently high, e.g. the 1.5%  $Mg_2Si$  alloy aged at 160°C after pre-aging at 40°C for 1 day, the dissolution may take place at  $T_2$ , but the more zones than those of after  $-20^\circ C$  quenching survive and continue to grow at  $T_2$ .

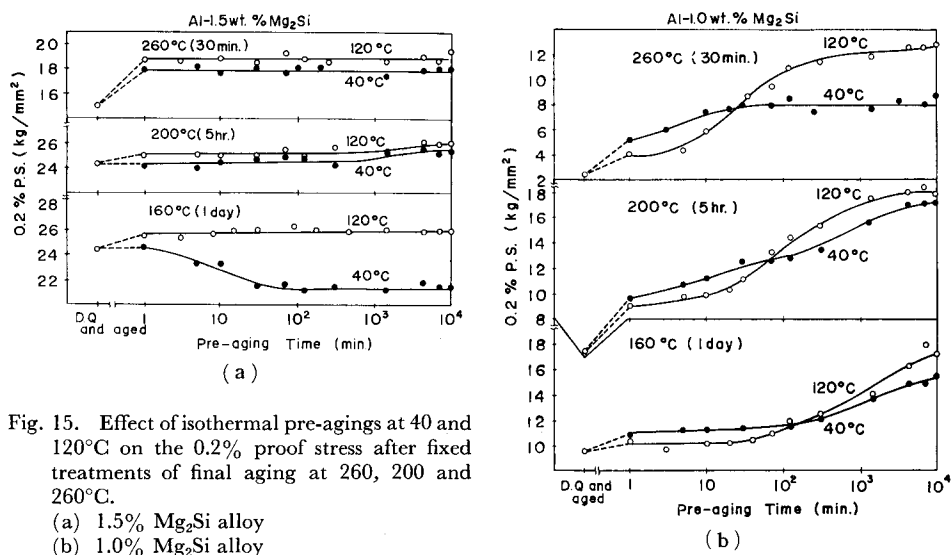


Fig. 15. Effect of isothermal pre-aging at 40 and 120°C on the 0.2% proof stress after fixed treatments of final aging at 260, 200 and 260°C.

- (a) 1.5%  $Mg_2Si$  alloy  
(b) 1.0%  $Mg_2Si$  alloy

The effect of isothermal pre-aging on the fixed final aging treatments are shown in Fig. 15. The periods of secondary aging are chosen to give the maximum proof stress at each temperature when the specimen of 1.5%  $Mg_2Si$  are directly quenched. In 1.5%  $Mg_2Si$  alloy, the change in the pre-aging time gives no effect on the final aging at 200 and 260°C. The value of proof stress is raised by pre-aging for 1 min at either 40°C or 120°C and the same value is observed for 1 week. However in final aging at 160°C, the proof stress decreases from the value of direct quenching with the pre-aging time at 40°C till ca. 50 min. and reaches an almost constant value there. It is interesting that the period coincides to the end of fast reaction in resistivity change as shown in Table 2. Photo. 4 shows the effect of pre-aging time at 40°C on the precipitation in 1.5%  $Mg_2Si$  alloy after final aging at 160°C for 1 day. The precipitates become coarser with the increasing pre-aging time. The pre-aging at 120°C for 2 hrs gives the similar fine structure as that of direct quenching, as shown in Photo. 5.

The longer pre-aging period is always corresponding to larger proof stress in the case of 1.0%  $Mg_2Si$  alloy. However, when compared to the value of  $-20^\circ C$  quen-

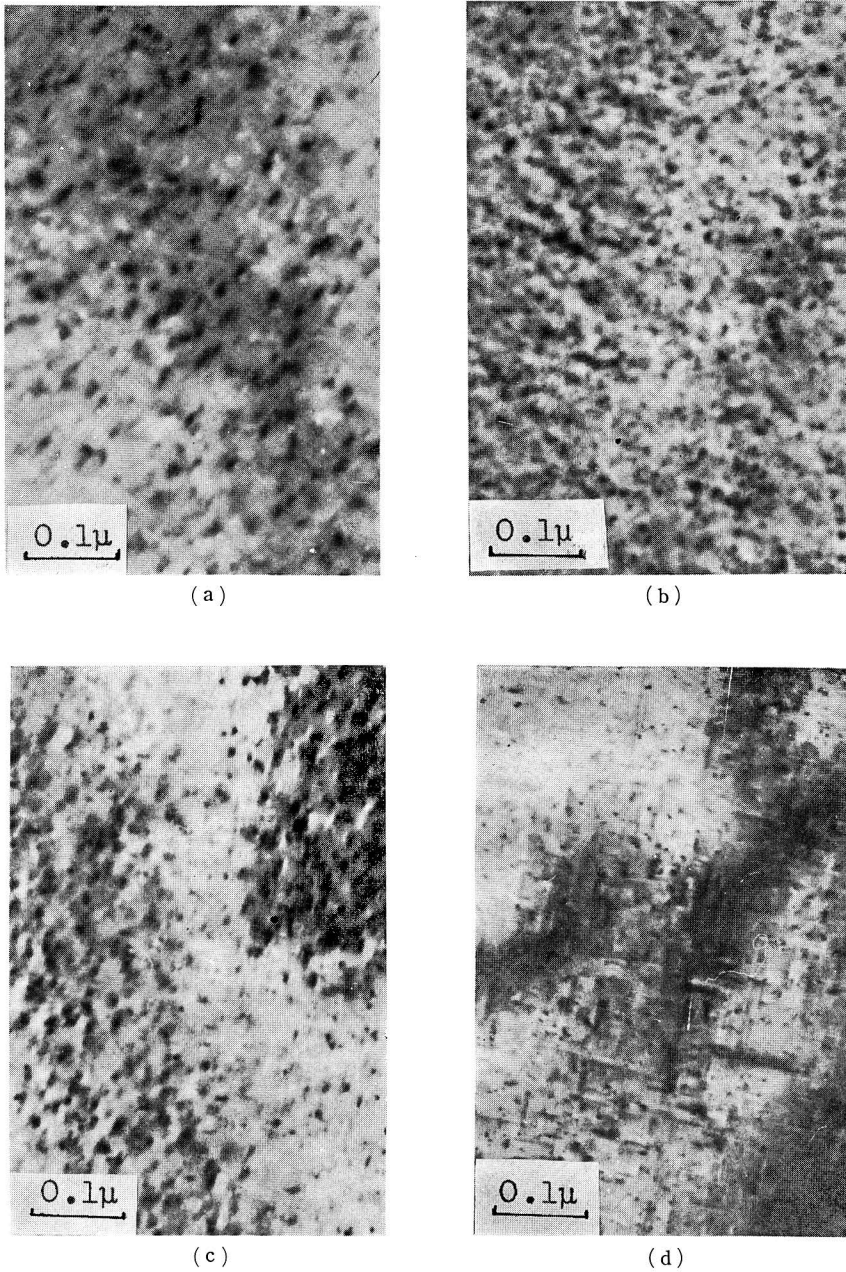


Photo. 4. The effect of pre-aging at 40°C on the precipitation in Al-1.5% Mg<sub>2</sub>Si alloy aged at 160°C for 1 day.  
(a) without pre-treatment, directly quenched to 160°C and aged for 1 day.  
(b) pre-aged at 40°C for 1 min.  
(c) pre-aged at 40°C for 10 min.  
(d) pre-aged at 40°C for 100 min.

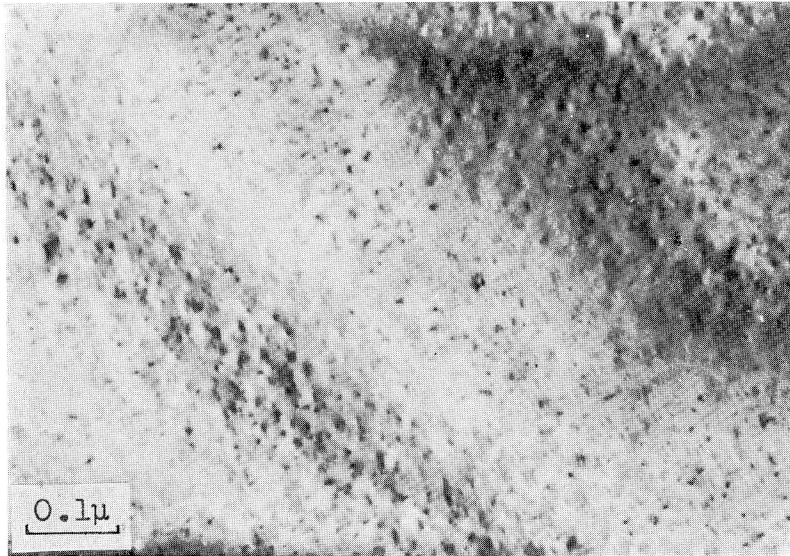
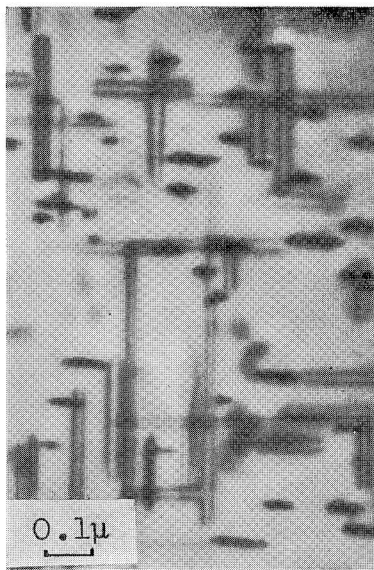
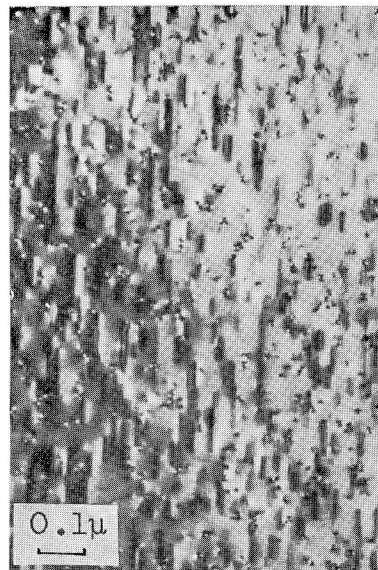


Photo. 5. The effect of pre-aging at 120°C for 2 hrs. on the precipitation in Al-1.5% Mg<sub>2</sub>Si alloy aged at 160°C for 1 day.



(a)



(b)

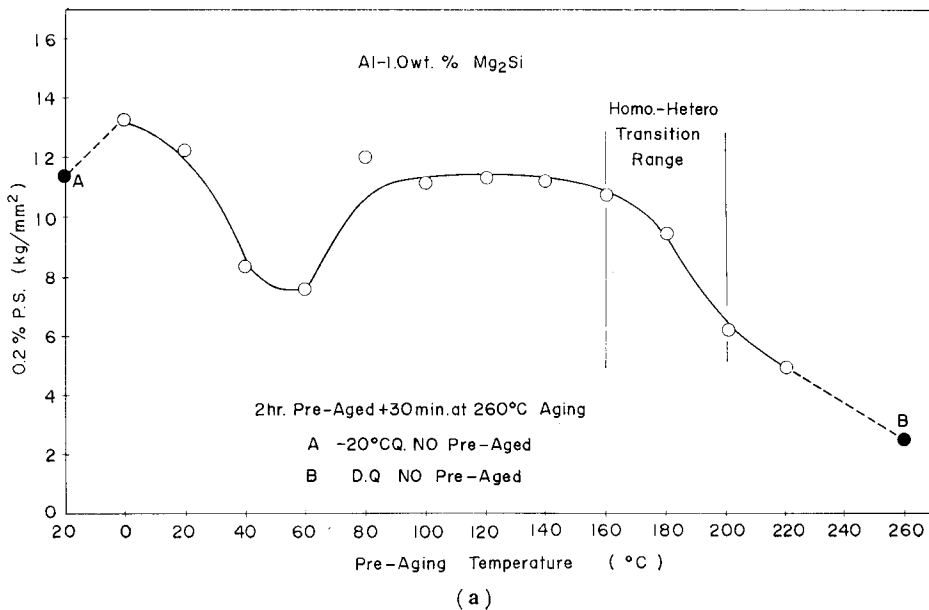
Photo. 6. The effect of pre-aging at 120°C on the precipitation in Al-1.0% Mg<sub>2</sub>Si aged at 200°C for 5 hrs.

- (a) pre-aged at 120°C for 10 min.
- (b) pre-aged at 120°C for 1000 min.



ching, the short pre-aging period gives a lower proof stress. Photo. 6 shows the effect of pre-aging time at 120°C on the aspect of precipitation after final aging at 200°C for 5 hrs. Finer structure is obtained by the pre-aging for a longer period in agreement with the change in proof stress. It is to be remembered that treatments of final aging are to give the maximum proof stress in 1.5% Mg<sub>2</sub>Si alloy directly quenched. Since these treatments is located before the maximum proof stress in 1.0% Mg<sub>2</sub>Si alloy, the lower value of proof stress means sometimes the larger retardation as shown in Fig. 14. The values of proof stress for various final aging after the longest pre-aging time in the present work are shown in Table 4 and 5, together with the values of no pre-aging.

The effect of isochronal pre-aging on the strength after final aging is investigated. Specimens are directly quenched and pre-aged for 2 hrs at each temperature between 0°C and  $T_2$  in steps of 20°C, then finally aged. The values of proof stress are shown in Fig. 16 as a function of pre-aging temperature together with the values after the -20°C and direct quenching. The 1.0% Mg<sub>2</sub>Si alloy finally aged at 260°C for 30 min, as shown in Fig. 16(a), gives a minimum value of proof stress at 60°C. The decrease above 160°C is explained by the decreased number of homogeneously nucleated precipitates by direct quenching to the pre-aging temperature. The high values below 40°C may be due to the inoculation effect as in the case of Al-1.0% Si alloy<sup>23</sup>). However, to explain the minimum at 60°C, one must consider the stability of pre-formed zones. Some results of direct observation



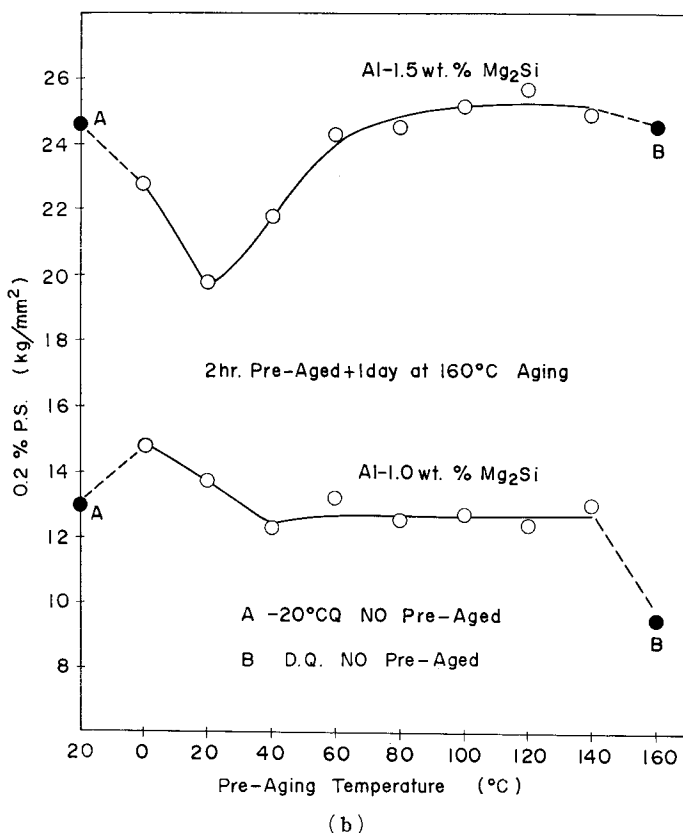
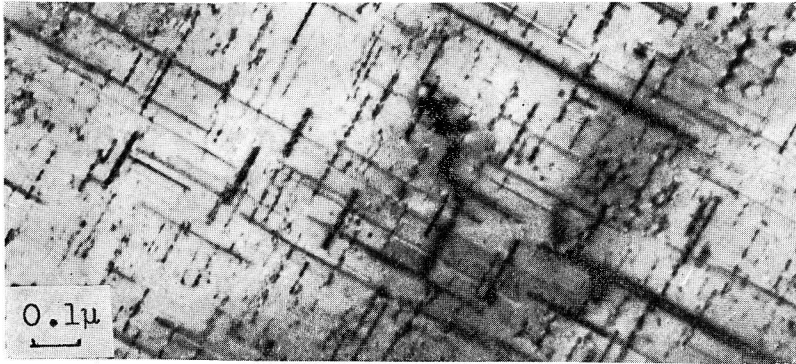


Fig. 16. Effect of isochronal pre-aging for 2 hrs. on the 0.2% proof stress after fixed treatments of final aging.

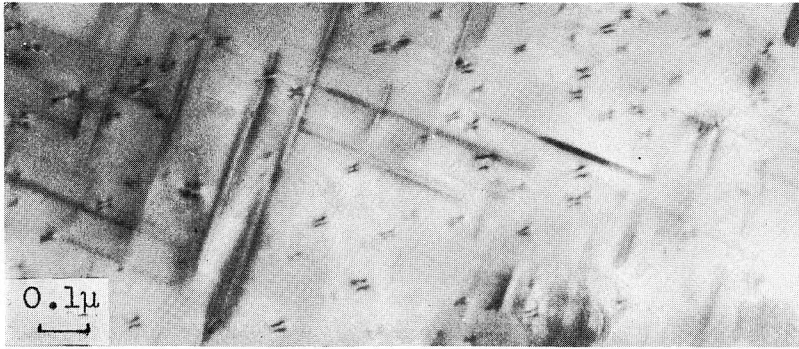
(a) 1.0% Mg<sub>2</sub>Si alloy finally aged at 260°C for 30 min.

(b) 1.0 and 1.5% Mg<sub>2</sub>Si alloys finally aged at 160°C for 1 day.

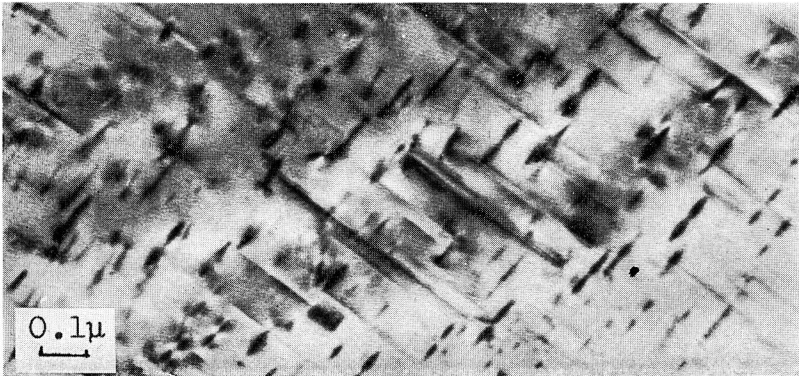
by electron microscope are shown in Photo. 7. The average length of needle-shaped precipitates becomes larger in the specimen pre-aged at 60°C for 2 hrs. As there is only a little retardation in isothermal curves of 1.0% Mg<sub>2</sub>Si alloy at 260°C after various treatments shown in Fig. 14(a), the retardation can not be the cause of decrease in proof stress. Thus, the decrease in number of zones, as shown in Photo. 7, must be caused by pre-aging. It is interesting that the aging for 2 hrs will give the resistivity maximum at the temperature between 60°C and 80°C which corresponds to the beginning of re-increase in proof stress. In the final aging at 160°C for 1 day as shown in Fig. 16(b), the 1.5% Mg<sub>2</sub>Si alloy shows similar decrease as 1.0% Mg<sub>2</sub>Si alloy aged at 260°C for 30 min, but the minimum appears at lower pre-aging temperature. Because the final aging temperature is lower than  $T_c$ , the decrease in this case may be considered as the result from the retardation. If the



(a)



(b)



(c)

Photo. 7. The effect of isochronal preaging for 2 hrs on the precipitation in Al-1.0% Mg<sub>2</sub>Si aged at 260°C for 30 min.  
(a) preaged at 0°C.  
(b) preaged at 60°C.  
(c) preaged at 120°C.

dissolution of excess number of zones takes place very slowly, the growth of survived zones may also proceed slowly owing to the low supersaturation. In 1.0%  $Mg_2Si$  alloy finally aged at 160°C for 1 day, the small increase in proof stress is observed below 40°C which should be due to the inoculation effect.

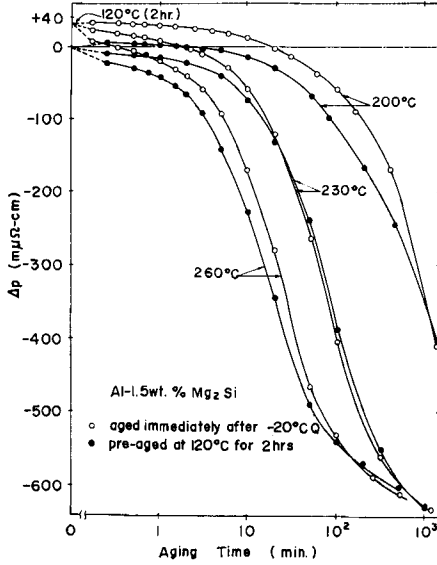


Fig. 17. Isothermal changes in resistivity of 1.5%  $Mg_2Si$  alloy aged at various temperatures after pre-aging at 120°C for 2 hrs. Compare with Figs. 13 and 14(a)

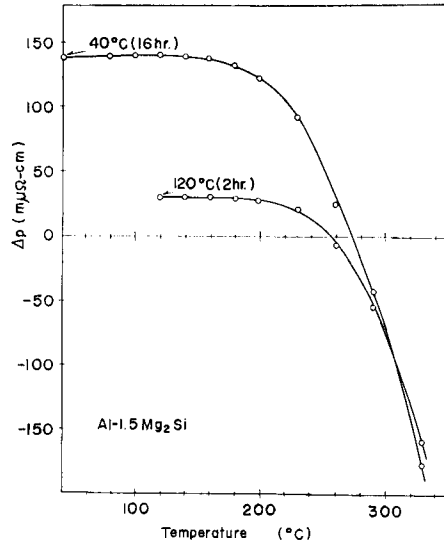


Fig. 18. Isochronal change in resistivity of 1.5%  $Mg_2Si$  alloy aged at each temperature for 1 min. after pre-aging at 120°C for 2 hrs., and at 40°C for 16 hrs. Compare with Fig. 2.

Figure 17 shows the isothermal changes in resistivity of 1.5%  $Mg_2Si$  alloy pre-aged at 120°C for 2 hrs. The resistivity of the pre-aged specimen is higher than that of non pre-aged one for considerably long aging periods. It is difficult to relate this fact directly to the increase in proof stress since the specimens for resistivity measurements and tensile tests have thermal histories different from each other. However, as the zones corresponding to the resistivity maximum contribute to the strengthening, it may be considered that the larger resistivity in pre-aged specimen suggests the smaller average size of zones. The results of isochronal aging after pre-aging are shown in Fig. 18. Though there is also a difference in thermal histories as in the case of Fig. 2, it can be said that the zones formed at 120°C are more stable than that of formed at 40°C.

### Conclusions

The re-dissolutions of clusters or small zones through two-step aging are

confirmed by resistivity measurements. For the decrease in resistivity at the initial stage of low temperature aging of 0.5% Mg<sub>2</sub>Si, two different contributions may be considered. One is the formation of vacancy-solute atom pair at the expense of single vacancies and the other is the re-dissolution at 20°C of clusters formed at -20°C. The former is proposed to the resistivity decrease in dilute Al-Ag alloys. In this case, the latter also seems to be probable since single vacancies should not remain through quenching.

The energy  $E_s$  for migration of solute atoms during the fast reaction was estimated as 0.77 eV for all three alloys in good agreement with the value reported for 1.4% Mg<sub>2</sub>Si alloy by Panseri and Federighi. However,  $E_{\max}$ , the apparent activation energy for resistivity maxima is strongly dependent on the alloy concentration. Comparing them each other the aging time corresponding to resistivity maximum  $t_{\max}$  for alloys aged at the same temperature, less  $t_{\max}$  is observed in the alloy of less concentration. This will be explained by the assumption of nearly equal concentration of quenched-in vacancies for all three alloys. Namely, the amount of diffusion during the fast reaction also may be equal and the concentration of Mg and Si atoms in solution at the end of fast reaction is higher, the higher is the alloy concentration. As shown by less value of  $t_s$  in high concentration alloy, the cluster number in the high concentration alloy is larger than that of the lower concentration alloy. Thus, if the resistivity maxima appears at a critical size of zones or clusters, the growth of individual zones requires longer periods to attain the critical size.

The critical temperature  $T_c$  for homogeneous nucleation of precipitates exists between 160 and 200°C in 1.0% Mg<sub>2</sub>Si alloy and between 200 and 260°C in 1.5% Mg<sub>2</sub>Si. The highest temperatures for each alloy at which the resistivity increase is observed are in the temperature ranges for  $T_c$ , respectively.

The specimens quenched directly to the aging temperature above  $T_c$  give less maximum proof stress at after the aging longer than that of quenched to -20°C. This observation means that the precipitates, whatever they may be, are nucleated at a temperature lower than  $T_c$ . It seems likely that the clusters formed during quenching and stabilized during heating to the aging temperature will facilitate the nucleation.

Assuming the same mechanism of precipitation hardening for pre-aged and not pre-aged specimens, the effect of two-step aging on the age-hardening in Al-Mg<sub>2</sub>Si alloys is explained as follows:

In the case that all clusters formed during pre-aging are finally dissolved, e.g. aging above  $T_c$  after short time pre-aging, the number of precipitates after final aging depends on the rate of dissolution. When the specimen is quenched to -20°C

or pre-aged at a sufficiently low temperature, the clusters may be too small to survive upto  $T_2$  and almost all of them will be dissolved rapidly. Thus the nucleation during heating will become ample to hardening nearly equal to the case of quenching to  $-20^\circ\text{C}$ . If the clusters are dissolved rather slowly, in the case of prolonged pre-aging, the nucleation will be suppressed by a less degree of supersaturation with the yet dissolving clusters. This explanation implicitly assumes the different precipitates at  $T_1$  and  $T_2$  respectively. This assumption seems to be valid because the decrease in proof stress, however slight it may be, is observed in isothermal aging at sufficiently high  $T_2$  after low temperature pre-aging. Further evidence needs to be given by experiment concerning the mechanism of strengthening. Such experiments are interesting since, if the ordered structure of zones reported by Lutts<sup>3)</sup> mainly contributes to the strength and the stability of zones are dependent on not only the zone size but also the degree of ordering, the effect of two-step aging may be more easily explained.

If the clusters or zones survived even at the final aging temperature, e.g. in the case of final aging at  $T_2$  below  $T_c$ , or high temperature pre-aging, the number of clusters may continue to grow slowly because the solute supersaturation must be sustained mainly by re-dissolution of smaller clusters. Therefore, the retardation occurs in isothermal age-hardening, and the strength after a fixed treatment of final aging becomes less than that of not pre-aged. However, after a prolonged pre-aging, the same value as that of not pre-aged is attained.

On an isochronal pre-aging, a minimum occurs in the proof stress after a fixed treatment of final aging. Therefore, the application of Becker's nucleation theory seems to be difficult in the case of two-step aging of Al-Mg<sub>2</sub>Si alloys

The present investigation was partially supported by a Research Fund provided by the Light Metal Educational Foundation, Inc. of Japan for which the authors wish to express their deep appreciation.

#### References

- 1) A.H. Geisler and J.K. Hill: Acta Cryst., **1** 238 (1948).
- 2) A. Guinier and H. Lambot: Acta Cryst. **1** 74, 227 (1948).
- 3) A. Lutts: Acta Met. **7** 741 (1959).
- 4) A. Saulnier and P. Miland: Rev. Met. **57** 91 (1960).
- 5) G. Thomas: J. Inst. Metals **90** 57 (1961-62).
- 6) D.W. Pashley, J. Rhodes and A. Sendorek: J. Inst. Metals **94** 41 (1966).
- 7) D.W. Pashley, M.H. Jacobs and J.T. Viets: Phil. Mag. **16** 51 (1967).
- 8) Y. Murakami, O. Kawano, S. Komatsu, T. Ohnishi and T. Nakazawa; Preprints for "International Conference on the Strength of Metals and Alloys" 1967, Tokyo, p. 226.
- 9) P.E. Fortin: Metal Prog. **89** 119 (1964).
- 10) J. Kats: Metal Prog. **89** 70 (1966).

- 11) M. Gnjatic: *Aluminium* **43** 442, 628 (1967).
- 12) G. Panseri and R. Federighi: *J. Inst. Metals* **94** 99 (1966).
- 13) G.W. Lorimer and R.B. Nicholson: *Acta Met.* **14** 1009 (1966).
- 14) R. Horiuchi and Y. Minonishi: *Preprints for 61st Conf. of JIM (Sapporo)* 136 (1967) (in Japanese).
- 15) K. Asano and K. Hirano: *Preprints for 61 st Conf. of JIM (Sapporo)* 131 (1967) (in Japanese).
- 16) H. Zoller and A. Ried: *Aluminium* **41** 626 (1965).
- 17) A. Guinier: *Solid State Physics* **9** 293 (1959).
- 18) W. Köster and G. Hofmann: *Z. Metalk.* **57** 819 (1966).
- 19) A. Kelly and R.B. Nicholson: "Progress in Material Science **10** 151 (1963) Pergamon Press
- 20) T. Federighi and G. Thomas; *Phil. Mag.* **7** 127 (1962).
- 21) M. Murakami: *Master Thesis, Kyoto University* (1968).
- 22) Y. Murakami, S. Komatsu and K. Nagata: *Mem. Fac. Eng. Kyoto Univ.* **29**(2) 161 (1967).
- 23) H.S. Rosenbaum and D. Turnbull: *Acta Met.* **6** 563 (1958).
- 24) C. Panseri and T. Federighi: *Acta Met.* **8** 217 (1960).
- 25) K. Asano and K. Hirano: *Trans JIM.* **9** 149 (1968).
- 26) C. Chiou, H. Herman and M.E. Fine: *Trans. Met. Soc. AIME* **218** 299 (1960).
- 27) H. Herman and M.E. Fine: *Trans, Met. Soc. AIME* **224** 503 (1962).
- 28) Y. Murakami and S. Komatsu: *Mem. Fac. Eng. Kyoto Univ.* in press.
- 29) W. Humerothery and G.V. Raynor: "The Structure of Metals and alloys" *Inst. Met. Monograph and Rept., No. 1* (1962) p. 183.